# HEAT TRANSFER WITH EVAPORATION AND BOILING OF A LIQUID IN POROUS BODIES

A. N. Abramenko, L. E. Kanonchik,
A. G. Shashkov, and V. K. Sheleg

UDC 536.423

The heat-transfer characteristics with evaporation and boiling of a liquid in porous evaporators when power is introduced under boundary conditions of the third kind are examined in this work.

The creation of new types of heat pipes requires detailed information concerning the heat-transfer characteristics in porous evaporators. The process of evaporation and boiling of a liquid in porous bodies is complicated and depends on many variables. Presently available experimental results are often contradictory. Decreasing the thickness of the porous body, according to data in [1, 2], intensifies heat removal, while according to data in [3], the opposite occurs. It was established in [4] that the thickness of the porous layer has no effect on the maximum heat flux density.

Experimental and theoretical works on heat exchange in porous evaporators are available for uniform heat input [1-5]. In constructing physical models, it was assumed that heat removal was uniform along the entire length of the porous body. However, for high heat flux densities, dried zones were observed to appear [5].

In practice, heat flux can be delivered to different heat-exchange setups with the help of fluid heat exchangers, i.e., under boundary conditions of the third kind. In this case, it cannot be asserted beforehand that heat removal is uniform over the entire length of the porous body. Based on this, it is useful to study experimentally porous evaporators in the case of heat transfer with boundary conditions of the third kind.

1. Porous Evaporators. Evaporators consisting of a porous body, baked onto a copper plate, were the object of the study. The porous body was obtained from OF-10-1 bronze powder with nearly spherical particles. The size of the particles is $(0.2\text{-}0.3)\cdot 10^{-3}$ m, the permeability of the evaporator is $7\cdot 10^{-12}$ m$^2$, the average radius of the pores is $6\cdot 10^{-5}$ m, and the overall porosity is 30%.

The heat flux was delivered to the porous evaporator with the help of a fluid heat exchanger (Fig. 1). Rubber packing was used to avoid heat transfer between the surface wall of the evaporator and the housing of the liquid heat exchanger. The working fluid (distilled water) was fed by two channels which drew the fluid from basins. The length of the evaporator is $10^{-1}$ m, the width is $5\cdot 10^{-2}$ m, the thickness of the porous body is $(0.65, 1, 2, 4)\cdot 10^{-3}$ m. The evaporator is placed horizontally. Along the length $x_0 = 10^{-2}$ m, the evaporator was in contact with the porous channel, while at $x_{max} = 4\cdot 10^{-2}$, it had an open surface for evaporation (boiling) of the fluid. The evaporator unit was placed in an experimental setup, which simulated the operation of a heat pipe [6].

2. Experimental Results and Their Analysis. During the course of the experiments, the dependence of the heat flux density on overheating of the evaporator wall above the saturation temperature was determined. Heat transfer between the dry walls of the evaporator unit and the surrounding medium was taken into account in measuring the no-load power. For small overheating (to 10°K), the porous body is completely wetted with fluid. Drops were not observed to be ejected from the structure. The temperature along the copper wall and the porous body is constant. As the overheating increases, a temperature differential appears along the length. The center of the porous body begins to dry out gradually. This is noticeable both by the jumplike increase in temperature and visually, since the dried segments differ in color from the wet segments. For maximum overheating, only the segments near the feeding channels remain completely wetted. Bubbles and spraying of fluid appear at the point of contact between the channels and the porous body.

The dependence of the heat flux density on the overheating of the wall is shown in Fig. 2. In our opinion, the mechanism for heat transfer with evaporation and boiling of the fluid in a porous body is as follows. For

A. V. Lykov Institute of Heat and Mass Transfer, Academy of Sciences of the Belorussian SSR. Institute of Applied Physics, Academy of Sciences of the Belorussian SSR. Belorussian Republican Scientific-Industrial Union for Powder Metallurgy, Minsk. Translated from Inzhenerno-Fizicheskii Zhurnal, Vol. 42, No. 2, pp. 218-227, February, 1982. Original article submitted March 23, 1981.

 0022-0841/82/4202-0144 $07.50 

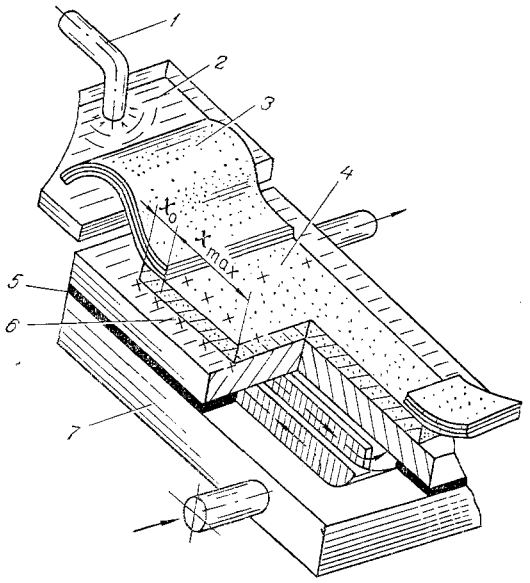


Fig. 1

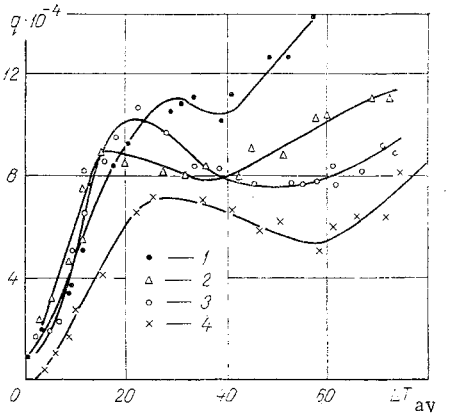


Fig. 2

Fig. 1. Evaporator unit: 1) connecting pipe; 2) basin; 3) porous channel; 4) porous evaporator; 5) packing; 6) thermocouple; 7) fluid heat exchanger.

Fig. 2. Dependence of the heat flux density on the overheating of the wall ($q \cdot 10^{-4}$, $W/m^2$; $\Delta T$, °K): 1) $h = 0.85 \cdot 10^{-3}$ m; 2) $10^{-3}$ m; 3) $2 \cdot 10^{-3}$ m; 4) $4 \cdot 10^{-3}$ m.

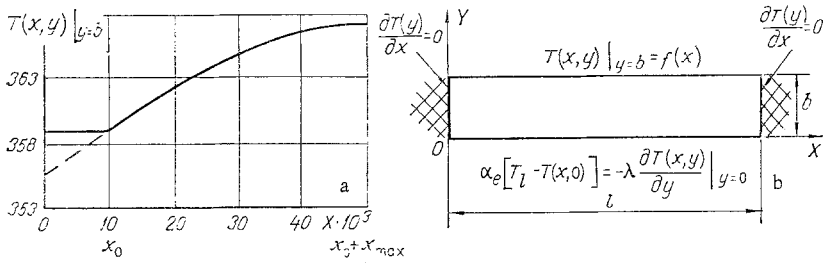


Fig. 3. Scheme for determining the local heat fluxes: a) change in temperature along the evaporator wall; b) boundary conditions on the wall; T, °K; X, m.

small overheating, heat is transferred through the porous body by conduction in the framework and the fluid layer, as well as by convection. The fluid will evaporate from menisci on the outer surface. Vapor is not formed inside the porous body. The temperature in the longitudinal direction both at the wall and at the porous body is constant. The evaporator ensures uniform heat removal.

When the temperature at the wall is increased above some limit ($\Delta T = 15°$), heat conduction and convection no longer remove the heat that is fed into the porous body. The fluid, which is in contact with the wall of the porous evaporator, begins to overheat, which leads to activation of the evaporation centers, appearance of bubbles, and creation of conditions for the onset of boiling. As the overheating increases, more evaporation centers are activated and the overall boiling area increases until it encompasses the entire surface of the evaporator wall. In view of the intensification of heat transfer, the heat flux, removed from different parts of the evaporator, begins to be determined by the amount of fluid permeating into that location. The heat flux begins to decrease from the hard-to-reach region: the center of the porous evaporator.

Since the inner surface of the evaporator, next to the copper wall, has the highest temperature, bubbles form in the porous body at that location. The vapor escapes to the outside through the largest pores. The fluid reaches the heated wall through the small pores. As the heat flux density increases, the vapor begins to fill the small-diameter pores, displacing fluid out of them. The heat flux, brought about by the evaporator, begins to drop. This is characterized on the curve $q = f(\Delta T)$ by the first inflection. Drying of the porous body is accompanied by an increase in its temperature, which decreases the contact angle of the working fluid. The con-

tact-breaking diameter of a bubble decreases to the characteristic pore size, i.e., vapor extraction improves. All of this causes the fluid to return into part of the pores of the evaporator and intensification of heat transfer. A new inflection appears in the curve $q=f(\Delta T)$. The evaporator heat flux density increased with increasing overheating up to the time that hydrodynamic limitations appeared in the fluid flow in the porous body.

The thickness and length of the porous body affect the maximum heat flux of the evaporator with other conditions remaining the same. The thicker the porous body, the greater is the mass flow velocity of fluid along the body. This encourages heat removal. On the other hand, the thicker the porous body, the greater is the temperature differential along it, which has a negative effect on evaporation. In the boiling regime, an increase in the thickness of the porous body inhibits vapor extraction. The experimental results showed that a porous evaporator with a thickness of $0.85 \cdot 10^{-3}$ m provides the highest heat flux (Fig. 2), i.e., the conditions for vapor extraction had a dominating effect on heat removal with boiling of fluid in the porous body.

3. Calculation of the Local Heat Fluxes. As indicated, for high heat flux densities, dried zones appear on porous bodies [5], which indicates nonuniformity in heat extraction along the length of the body. In order to determine analytically the maximum heat flux density that can be removed by a porous evaporator under boundary conditions of the third kind, it is necessary to clarify the nature of heat removal along the porous body. During the course of the experimental investigation of porous evaporators, the temperature field was measured along the copper substrate, on which porous bronze was baked (Fig. 1). Visual observations and the results of measurements show that for maximum heat removal, the segment $x_0$ is completely wetted by liquid and the temperature on it is constant; on the segment $x_{max}$, the degree of drying and the temperature increased with increasing distance from the location at which the fluid was injected. Since the heat conduction of a porous body depends on the degree to which it is filled with fluid and is not constant along the length of the body, the calculation of local heat flux was based on the change in the temperature of the upper surface of the copper substrate. The experimental data were approximated by a polynomial on a computer using the method of least squares. The functional dependence for T and x was found in the form (Fig. 3a):

$$T(x) = Ax^2 + Bx + C. \tag{1}$$

Taking into account the fact that the temperature differential between the water entering and leaving the fluid heat exchanger did not exceed 0.5°K, it may be assumed that the temperature is constant ($T_l$ = const). The average heat-transfer coefficient in the channel of the fluid heat exchanger was calculated according to [7] for turbulent flow of the heat-transfer agent (Re = 27900) and equaled $\alpha = 10^4$ W/m$^2 \cdot$ K. Measurements of the temperature (Fig. 1) in the transverse cross section of the porous body made it possible to assume that $\partial T/\partial z = 0$. Then, the differential heat-conduction equation for a copper wall is written as follows:

$$\frac{\partial^2 T(x,\ y)}{\partial x^2} + \frac{\partial^2 T(x,\ y)}{\partial y^2} = 0. \tag{2}$$

The boundary conditions are (Fig. 3b):

1) the temperature on the upper surface of the wall (y = b) is

$$T(x,\ y)|_{y=b} = Ax^2 + Bx + C;$$

2) heat transfer at the lower surface of the wall (y = 0) is

$$-\lambda \left.\frac{\partial T(x,\ y)}{\partial y}\right|_{y=b} = \alpha [T_l - T(x,\ y)]; \tag{3}$$

3) heat transfer on the lateral surfaces of the wall (x = 0; x = $l$) is

$$-\lambda \left.\frac{\partial T(x,\ y)}{\partial x}\right|_{x=0} = 0; \quad -\lambda \left.\frac{\partial T(x,\ y)}{\partial x}\right|_{x=l} = 0.$$

In order to solve the partial differential equation (2), we used the Fourier cosine transformation. Knowing the temperature distribution T(x, y), it is possible to find the local heat flux removed on the segment from $x_i$ to $x_{i+1}$ under given boundary conditions:

$$Q_i = w \int_{x_i}^{x_{i+1}} -\lambda \left.\frac{\partial T(x,\ y)}{\partial y}\right|_{y=b} dx = w \left\{ \frac{T_l - \frac{Al^2}{3} - \frac{Bl}{2} - C}{\frac{1}{\alpha} + \frac{b}{\lambda}} (x_{i+1} - x_i) - \right.$$

$$-4\frac{\lambda}{l}\left[\sum_{n=1}^{\infty} D_n \cos\frac{n\pi}{l}\frac{(x_{i+1}+x_i)}{2}\sin\frac{n\pi}{l}\frac{(x_{i+1}-x_i)}{2}\right]\Bigg\}; \tag{4}$$

$$D_n=\frac{\operatorname{ch}\frac{n\pi}{l}b+\frac{\lambda n\pi}{\alpha l}\operatorname{sh}\frac{n\pi}{l}b}{\frac{\lambda n\pi}{\alpha l}\operatorname{ch}\frac{n\pi}{l}b+\operatorname{sh}\frac{n\pi}{l}b}\left[2A\left(\frac{l}{n\pi}\right)^2\cos n\pi+B\left(\frac{l}{n\pi}\right)^2\cos n\pi-B\left(\frac{l}{n\pi}\right)^2\right].$$

The local heat fluxes were calculated using Eq. (4) for porous bodies with different thicknesses. The change in local heat fluxes on the segment from $x_0$ to $x_0+x_{max}$ is described by a quite complicated function. For convenience, the computed curve can be approximated with adequate accuracy by a simple function of the form

$$\frac{dQ}{dx}=\frac{B'}{x^2}.$$

Then, the magnitude of the heat flux, removed with a phase transition in the porous body, can be represented as the area bounded by the coordinate axes and the curve $B'/x^2$. The heat flux on the segment from 0 to $x_0$ is

$$Q_0=B/x_0,$$

while on the segment from $x_0$ to $x_0+x_{max}$

$$Q_x=\int_{x_0}^{x_0+x_{max}}\frac{B'}{x^2}dx=\frac{B'x_{max}}{x_0(x_0+x_{max})}.$$

4. Derivation of Working Equations for Maximum Heat Flux. In deriving the working equations for determining the maximum heat flux, removed by a porous evaporator, the following conditions were assumed:

1) the fluid moves in the porous body due to surface tension forces;

2) the fluid practically completely wets the material of the porous body;

3) the segment of the evaporator with length $x_0$ is completely saturated by fluid, and constant heat removal is established on it;

4) on the free segment of the evaporator with length $x_{max}$, the nature of the heat removal is approximated by the function $B'/x^2$;

5) in any cross section of the porous body, the change in capillary pressure equals the increase in drag;

6) at the point $X=x_0$, the contact angle is maximum: $\theta=90°$; at the point $X=x_0+x_{max}$, the contact angle is minimum: $\theta=0°$.

Evaporator Segment with Length $x_0$. The equation for balance of pressure in the porous body is

$$\frac{dP_{cap}}{dx}=-\frac{dP_h}{dx}. \tag{5}$$

The change in drag is described by Darcy's law

$$dP_h=\frac{\dot{m}(x)\mu_l}{\rho KA(x)}dx, \tag{6}$$

where $A(x)=wh$; $\dot{m}(x)=0.5Q/r^*$ (the coefficient 0.5 is introduced due to the uniform input of fluid into the porous body along the segment $x_0$).

The change in the capillary pressure in the porous body is

$$dP_{cap}=-\frac{2\sigma}{R_{cap}}\sin\Theta d\Theta. \tag{7}$$

Then, the heat flux on the segment $x_0$ is found by integrating (5) taking into account (6) and (7):

$$\int_{\Theta=90°}^{\Theta=\Theta_0}\frac{2\sigma}{R_{cap}}\sin\Theta d\Theta=\int_0^{x_0}\frac{\mu_l Q_0}{2KA(x)r^*\rho}dx,$$

$$Q_0 = \frac{4N_l\, Kwh \cos\Theta_0}{x_0 R_{cap}}, \tag{8}$$

where

$$N_l = \sigma\rho r^*/\mu_l . \tag{9}$$

Evaporator Segment with Length $x_{max}$. In this case, in Eq. (6), the terms $\dot{m}(x)$ and $A(x)$ vary along the evaporator. For $X = x_0$ and $A(x) = wh$,

$$\dot{m}(x_0) = \frac{Q_x}{r^*} = \frac{B' x_{max}}{r^* x_0 (x_0 + x_{max})} . \tag{10}$$

With the onset of maximum heat removal, all of the fluid fed into the evaporator evaporates along the porous body and, in addition, at the section $X = x_0 + x_{max}$, the area of the transverse layer of fluid $A(x) = 0$.

The mass consumption of fluid in any section x is

$$\dot{m}(x) = \frac{B'}{r^*}\left[\frac{x_{max}}{x_0 (x_0 + x_{max})} - \frac{x}{x_0 (x_0 + x)}\right]. \tag{11}$$

At the same time,

$$\frac{B' x_{max}}{x_0 (x_0 + x_{max})} = Q_x . \tag{12}$$

Finally,

$$\dot{m}(x) = \frac{Q_x}{r^*}\left[1 - \frac{x (x_0 + x_{max})}{x_{max} (x_0 + x)}\right]. \tag{13}$$

The area of the fluid flux in any section of the porous body is $A(x) = wd(x)$, $d(x) = h - h(x)$. The part of the porous body with length $x_{max}$ is separated into m elementary segments (Fig. 4). The volume of the fluid evaporated in the first elementary segment is:

$$V_1' = \frac{B'\tau}{\rho r^*} \frac{x_1}{(x_0 + x_1) x_0} .$$

The volume of fluid evaporated in the i-th segment is:

$$V_i' = \frac{B'\tau}{\rho r^*} \frac{x_i - x_{i-1}}{(x_0 + x_{i-1})(x_0 + x_i)} .$$

The volume of the porous body occupied by vapor in the first segment equals the volume of the evaporating fluid in this segment; in the second, it equals the sum of the volumes of fluid evaporating in the first and second segments, etc. In the general case, the volume of the porous body filled with vapor at the i-th segment is:

$$V_i = \frac{B'\tau}{\rho r^*}\left[\frac{x_1}{x_0 (x_0 + x_1)} + \ldots + \frac{x_i - x_{i-1}}{(x_0 + x_{i-1})(x_0 + x_i)}\right]. \tag{14}$$

The vapor volume in the n segments of the porous body is

$$V_n = \sum_{i=1}^{n} V_i = \frac{B'\tau}{\rho r^*}\left[\frac{x_1 n}{x_0 (x_0 + x_1)} + \sum_{i=2}^{n} \frac{(x_i - x_{i-1})(n - i + 1)}{(x_0 + x_{i-1})(x_0 + x_i)}\right]. \tag{15}$$

The vapor volume in the part of the porous body with length $x_{max}$ is

$$V_{max} = \frac{B'\tau}{\rho r^*}\left[\frac{x_{max}}{x_0 (x_0 + x_1)} + \sum_{i=2}^{m} \frac{(x_i - x_{i-1})(m - i + 1)}{(x_0 + x_{i-1})(x_0 + x_i)}\right]. \tag{16}$$

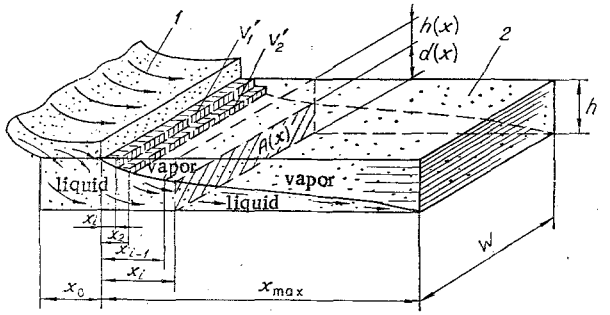


Fig. 4. The fluid flow in a porous body (working model): 1) channel; 2) porous body.

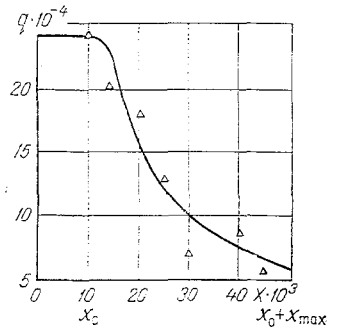


Fig. 5. Dependence of the maximum heat flux density on the length of the porous body ($q_{max} \cdot 10^{-4}$, W/m$^2$; $X \cdot 10^3$, m): the points show the experimental values; the curve shows the computed values.

On the other hand (Fig. 4):

$$V_n = \mathrm{Kp}\, wxh(x)\,\varepsilon, \tag{17}$$

$$V_{max} = \mathrm{Kp}\, wxh\varepsilon. \tag{18}$$

Simultaneous solution of Eqs. (15)-(18) permits determining the quantity h(x):

$$h(x) = h\,\frac{x_{max}}{x}\left[\frac{\dfrac{x_1 n}{x_0(x_0+x_1)} + \sum_{i=2}^{n}\dfrac{(x_i - x_{i-1})(n-i+1)}{(x_0+x_{i-1})(x_0+x_i)}}{\dfrac{x_{max}}{x_0(x_0+x_1)} + \sum_{i=2}^{m}\dfrac{(x_i - x_{i-1})(m-i+1)}{(x_0+x_{i-1})(x_0+x_i)}}\right]. \tag{19}$$

After substituting expressions (13) and (19) into Eq. (5), it takes the form

$$\frac{2\sigma}{R_{cap}}\int_{\Theta=\Theta_0}^{\Theta=0}\sin\Theta d\Theta = \frac{Q_x}{K\rho}\,\frac{\mu_{ж} I}{r^* wh},$$

where

$$I = \int_0^{x_{max}} \frac{\left[1 - \dfrac{x(x_0+x_{max})}{(x_0+x)\,x_{max}}\right]dx}{1 - \dfrac{x_{max}}{x}\left[\dfrac{\dfrac{x}{x_0(x_0+x_1)} + \sum_{i=2}^{n}\dfrac{(x_i - x_{i-1})(n-i+1)}{(x_0+x_{i-1})(x_0+x_i)}}{\dfrac{x_{max}}{x_0(x_0+x_1)} + \sum_{i=2}^{m}\dfrac{(x_i - x_{i-1})(m-i+1)}{(x_0+x_{i-1})(x_0+x_i)}}\right]}. \tag{20}$$

The final equation for the maximum heat flux in the evaporator segment with length $x_{max}$ is

$$Q_x = \frac{2N_l\, Kwh}{fR_{cap} I}\,(1 - \cos\Theta_0), \tag{21}$$

where f is a coefficient that takes into account the effect of the phase transition on the motion of the fluid in the porous body. From the experimental results, we determined the values of the angle $\Theta_0 = 85.9°$ and coefficient f: for $h \cdot 10^{-3}$ m equal to 4, 2, 1, and 0.85, f equals 40, 24.5, 18.5, and 16, respectively.

The maximum heat flux extracted by the porous evaporator is

$$Q_{max} = Q_0 + Q_x$$

or

$$Q_{\max} = \frac{2N_l\, Kwh}{R_{\text{cap}}}\left[\frac{2\cos\Theta_0}{x_0} + \frac{1-\cos\Theta_0}{fI}\right]. \tag{22}$$

The maximum heat flux density is

$$q_{\max} = \frac{2N_l\, Kh}{x_{\max}R_{\text{cap}}}\left[\frac{2\cos\Theta_0}{x_0} + \frac{1-\cos\Theta_0}{fI}\right]. \tag{23}$$

The results of the calculation and experiment for a porous body with thickness $4\cdot10^{-3}$ m and length varying from $10^{-2}$ to $5\cdot10^{-2}$ m are shown in Fig. 5. The mean-square deviation of the computed data from the experimental data was 5.8%.

## NOTATION

A(x), area of the transverse layer of fluid in the porous body at section x; A, area of the transverse cross section of the porous body; A, B, C, and B', coefficients; b and w, geometric parameters of the porous evaporator; d(x), height of the fluid layer in the porous body at section x; h(x), height of the vapor layer in the porous body in section x; I, a definite integral; Kp, a coefficient that takes into account the distortion of the volume occupied by the vapor; $l$, length; $\dot{m}$, mass flux of the fluid; $N_l$, characteristic of the working fluid; P, pressure; Q, heat flux; $Q_0$, heat flux, provided by the porous evaporator at the segment $x_0$; $Q_x$, heat flux, provided by the porous evaporator on the segment from $x_0$ to $x_0+x_{\max}$; q, heat flux density; R, radius; $r^*$, latent heat of vaporization; T, temperature; x, y, and z, coordinates; $V'_i$, volume of the fluid, evaporating in the i-th segment; $V_i$, volume of the porous body, filled by vapor in the i-th segment; K, permeability; $\alpha$, heat-transfer coefficient; $\Theta$, contact angle; $\lambda$, thermal conductivity; $\mu$, viscosity; $\sigma$, surface tension; $\varepsilon$, porosity; $\tau$, time; the indices are: h denotes hydraulic; $l$ denotes liquid; cap denotes capillary; max denotes maximum; i is an order number; x indicates the cross section of the porous body.

## LITERATURE CITED


1. V. I. Tolubinskii, V. A. Antonenko, and Yu. N. Ostrovskii, "Heat-transfer mechanism and characteristics of vaporization in the evaporation zone of a heat pipe," Izv. Akad. Nauk SSSR, Energ. Transport, No. 1, 141-148 (1979).
2. V. A. Dyundin, G. N. Danilova, and A. V. Borishanskaya, "Heat transfer with boiling of refrigerants on surfaces of porous coatings," in: Heat Transfer and Hydrodynamics [in Russian], Nauka, Leningrad (1977), pp. 15-30.
3. A. P. Ornatskii, M. G. Semena, and V. I. Timofeev, "Experimental investigation of maximum heat fluxes on flat metal fiber wicks under typical conditions in heat pipes," Inzh.-Fiz. Zh., 5, No. 5, 782-788 (1978).
4. V. A. Afanas'ev and B. F. Smirnov, "Investigation of heat transfer and limiting heat fluxes with boiling in capillary porous structures," Teploenergetika, No. 5, 65-67 (1979).
5. A. Abkhat and R. Seban, "Boiling and evaporation of water, acetone, and ethyl alcohol in heat pipe wicks," Teploperedacha, 96, No. 3, 74-82 (1974).
6. L. L. Vasil'ev, A. N. Abramenko, and L. E. Kanonchik, "Heat transfer with evaporation and boiling of a liquid in grooves in thin-film evaporators," Raketn. Tekh. Kosmon., 17, No. 12, 110-118 (1979).
7. M. A. Mikheev and I. M. Mikheeva, Fundamentals of Heat Transfer, Beekman Publ. (1968).